Preprint
UCRL-JC-146832

Observation of a Hydrodynamically-Driven, Radiative-Precursor Shock

P.A. Keiter, R.P. Drake, T.S. Perry, H. Robey, B.A. Remington, C.A. Iglesias, R.J. Wallace, and J. Knauer

This article was submitted to Physics Review Letters

January 15, 2002

U.S. Department of Energy

Lawrence Livermore National Laboratory

Observation of a Hydrodynamically-Driven, Radiative-Precursor Shock

P. A. Keiter, R. P. Drake

University of Michigan, Ann Arbor, MI.

T. S. Perry, H. Robey, B. A. Remington, C. A. Iglesias, R. J. Wallace

Lawrence Livermore National Laboratory, Livermore, CA.

J. Knauer

Laboratory for Laser Energetics, University of Rochester, Rochester, NY.

ABSTRACT

Observations of a radiative-precursor shock that evolves from a purely hydrodynamic system are presented. The radiative precursor is observed in low-density SiO_2 aerogel foam using x-ray absorption spectroscopy. A plastic slab, shocked and accelerated by high-intensity laser irradiation, drives the shock, which then produces the radiative precursor. The length and temperature profile of the radiative precursor are examined as the intensity of the laser is varied.

A radiative-precursor shock occurs when the flux of ionizing photons being radiated forward from the shock front exceeds the flux of atoms approaching the shock front. This requires that the shock velocity exceed the threshold required to produce the necessary photon flux. The radiative precursor heats the medium ahead of the density discontinuity to a temperature approximately equal to the temperature at the forward shock front. Radiative-precursor shocks are relevant to astrophysics, for example in supernova [1], supernova remnants [2,3] and jets [4,5,6].

Here we report measurements of the temperature profile in a radiative precursor shock, deliberately produced to be suitable for modeling by simulations. In particular, one goal was to produce a radiative precursor shock that may be used to test current astrophysical codes. To do this, two criteria must be met. There must be a purely hydrodynamic intermediate state after the laser pulse. Astrophysical codes do not and should not try to model laser absorption physics. In this experiment, shocking a plastic slab and letting it expand into a vacuum gap achieve this goal. This allows the system to obtain a hydrodynamic state from which the radiative effects arise. There must also be temperature profile measurements to compare to the code predictions. This is achieved in the experiment by means of x-ray crystal spectrometry.

In related prior work, UV emission was observed when a radiative precursor reached a gold obstacle in a xenon shock tube [7]. This prior experiment provided evidence that the phenomenon exists but was not very suitable for detailed study as the small laser spot led to very complex hydrodynamics and the diagnostic did not produce data regarding the structure of the precursor [8]. Other related work has included studies of the transport of radiation from an x-ray source into a low-density medium [9] and studies of blast waves in gases that involve electron heat conduction and radiative heat transport [10].

In this Letter, we report direct observations of such a hydrodynamically-driven, radiative-precursor shock. The radiative precursor is observed using x-ray absorption spectroscopy. Comparing the observed silicon absorption to simulated spectra yields a temperature profile of the radiative precursor. The peak temperature and the length of the radiative precursor from the shock are found to depend on the drive beam power. Evidence of a threshold shock velocity to produce a radiative precursor is also presented.

The targets consist of a sequence of layers. A 60 μm slab of 1.2 g/cm^3 polycarbonate plastic is followed by a 150 μm vacuum gap, and then by 2000 μm of SiO_2 aerogel foam. The density of the foam was varied from 5 mg/cm^3 to 15 mg/cm^3, however for the cases examined here the foam density is 9.6 mg/cm^3. The targets are contained in an Au tube of 600 μm square cross section. The tube has two 400 μm by 1500 μm windows to allow diagnostic access. Across one window is a gold grid. A fiducial wire is placed 400 μm from the grid. These spatially calibrate the data. Extensive shielding prevents laser light and plasma from the irradiated surface from interacting with the other target components. A schematic of the experimental setup is shown in Figure 1. Ten beams of the OMEGA laser are incident on the plastic, with 1ns square pulses and beam energies that are varied from 400 J/beam to 500 J/beam. These drive beams use distributed phase plates to produce a super-Gaussian spatial profile with the intensity of each beam given by $I\ (W/cm^2) = (E/500) \times 8.5\times10^{13} \exp[-(r/412\ \mu m)^{4.7}]$, where E is the energy of the beam in J. Six beams with a 200 ps pulse length strike a thulium backlighter to provide diagnostic x-rays. The x-rays are dispersed with a KAP crystal spectrometer ($2d = 25.9\,\mathring{A}$) and recorded onto Kodak DEF film. The spectrometer is configured to include the silicon K-edge and 2p and 3p absorption lines in its spectral range (1.6 – 2.1 keV). The backlighter beams are delayed 5.5 ns from the main drive beams unless stated otherwise. The spectrometer entrance aperture is positioned 8 mm from the object position, which is centered at 850 μm from the target chamber center.

The temperature profile of the radiative precursor is constructed by comparing experimental and theoretical transmission spectra of silicon. This method for inferring the temperature has been successfully tested in earlier experiments under similar matter conditions [11]. The calculations are performed with the OPAL code [12], which uses an activity expansion method to determine the level populations. The atomic data required to generate the spectrum is obtained by solving a spin-averaged Dirac equation for parametric potentials which were pre-fitted to experimental results. The accuracy is comparable to single-configuration self-consistent-field calculations and should be sufficient considering the spectral resolution of the present experiment. The HYADES 1-D [13] code is used to simulate the experiments and to compare to the data. The version of HYADES used for the simulations of these experiments is a Lagrangian, radiation hydrodynamics code that uses greybody opacity and flux-limited, diffusive heat transport by electrons and radiation.

Figure 2a is an example of a typical radiograph with silicon absorption lines present. The foam density is 9.6 mg/cm^3 and the peak drive beam irradiance is 8.5 x 10^{14} W/cm^2. The forward shock is travelling from the left side to the right side of the image. Region I extends from the left edge of the image to the shock front and consists of shocked foam. If the image extended further left, then behind the shocked foam, shocked plastic would be observed. Region II extends from the shock front to the dashed line and includes the gold grid. This region consists of ionized but unshocked foam and is referred to as the radiative precursor. The 'boundary' between regions II and III is determined by the observable extent of the silicon absorption lines. The feature centered roughly at 1030 μm is visible on all of the data and due to a defect in the crystal. Region

III extends from the dashed line to the right hand edge of the film. This region consists of unshocked, unheated foam. The gold wire is also present in this region. Noted in the figure are the location of the 1s-3p absorption lines and some of the 1s-2p absorption lines, including the F-like, O-like, N-like, C-like and B-like. Also noted on the figure is the position of the silicon K-edge. Figure 2b shows three absorption spectra taken at different spatial locations. The spectra are offset vertically from each other to make viewing the easier. At positions farther from the forward shock, the number of absorption features in the spectrum decreases. This indicates a temperature gradient in the radiative precursor region. The temperature profile will be discussed in more detail later.

Figure 3 presents the density profile from a HYADES simulation using the experimental parameters of the data shown in Figure 2. As seen in Figure 2, the position of the forward shock is roughly 640 μm. This measurement differs from the HYADES simulation by less than 1%, indicating excellent, indeed perhaps fortuitous, agreement. We attribute the flat shelf behind the shocked foam to the rarefaction of the leading edge of the plastic slab, which can form such a shelf as described for example in Zeldovich and Razier. [14]

Figure 4 compares the temperature profile predicted by the HYADES code with the experimentally determined temperature profile for the conditions previously described. Clearly, there is a large discrepancy between the experiment and the simulation results. HYADES predicts a much higher temperature for the radiative precursor region. Experimentally, the temperature is highest at the forward shock and then quickly decreases in magnitude. The foam is heated to a couple of eV out to roughly

950 μm, suggesting the radiative precursor extends for about 300 μm. This estimate is also less than the HYADES prediction of 500 μm.

The length of the radiative precursor depends sensitively on the laser drive power, among other parameters. By decreasing the drive beam laser intensity from 8.5 x 10^{14} W/cm^2 to 7.3 x 10^{14} W/cm^2 while keeping all other parameters constant, the radiative precursor decreases in length and temperature. The experimentally measured temperature profile is much less than that predicted by HYADES and the length of the radiative precursor is also less than predicted by HYADES. The data indicate that increasing the laser drive will increase both the peak temperature and the length of the radiative precursor. Although the temperature profiles predicted by HYADES do not agree with the experiments, the general trend of a larger radiative precursor with a greater laser drive power is upheld.

By lowering the laser drive power sufficiently, the radiative precursor is not observed. In another experiment, the target used a 100 um plastic slab, the laser drive irradiance was 3.4x10^{14} W/cm^2, the foam density was 5 mg/cm^3 and the backlighter timing was 8 ns. Figure 5 compares the experimentally measure profile to the HYADES prediction. For these parameters, a small radiative precursor is observed with a peak temperature of only a few eV and extending roughly 100 microns ahead of the forward shock. There is a large discrepancy between the experiment and HYADES predictions.

A simple estimate of the minimum shock velocity required to produce a radiative precursor is presented here. A radiative precursor will be present if the number of ionizing photons radiated from the shock front exceeds the number atoms approaching the shock front. The electron and ion temperatures are assumed to be equal, and only temperatures well above the ionization energy are considered. The flux of photons is found, by integrating over the Plank distribution, to be $2.4x10^{23}\varepsilon T_{\mathrm{eV}}^{3} \geq \left(\rho/\left(Am_{p}\right)\right)\mathrm{v}_{s}$, where T_{eV} is the electron/ion temperature in eV, ε is the emissivity, ρ is the density, A is the average atomic mass per ion and m_p is the proton mass. For an ionic charge, Z, the temperature is related to the shock velocity, v_s, by the modified standard relation,

$$T_{\mathrm{eV}} = \frac{3}{16}\frac{Am_p}{(Z+1)}\frac{\mathrm{v}_s^2}{\left(1.6\times 10^{-12}\right)}.$$

Substituting and solving for v_s yields a threshold shock velocity for when a radiative precursor is produced

$$\mathrm{v}_s \geq 510\left(\frac{(Z+1)^{3/5}}{A^{4/5}}\right)\left(\frac{\rho}{\varepsilon}\right)^{1/5} \text{ km/s.}$$

Although the shock velocity is not directly measured in these experiments, it can be estimated from the HYADES simulations. The shocked material is optically thick so $\varepsilon \sim 1$. For the experimental parameters, the minimum shock velocity required for the ionization of 3 that corresponds to the lower-irradiance experiment is

$$\mathrm{v}_s \geq 67\text{km/s.}$$

For the higher laser irradiance experiments, HYADES predicts shock velocities of approximately 100 km/s. However, for the lower laser irradiance experiments, HYADES predicts a shock velocity of approximately 60 km/s. Comparing the velocities from these predictions to the threshold velocity, a radiative precursor should be seen in the higher irradiance case while one should not be observed in the lower irradiance case. Qualitatively the data supports this even without shock velocity measurements.. However, there is still significant disagreement between the temperature profiles of the experiments and the simulations. More detailed measurements of the shock velocity and the threshold behavior of the radiative precursor are planned.

In summary, a radiative-radiative precursor shock has been observed in a hydrodynamically-driven system. The peak temperature and the length of the radiative precursor depend on the laser drive power. Although the temperature profiles do not fit the predictions of the HYADES simulations, the general trend of a larger radiative precursor with greater laser drive power is upheld. The data also suggests there is a threshold shock velocity needed to produce a radiative precursor. The experimental data is consistent with an analytic approximation of the threshold shock velocity. A more detailed study of this threshold is needed to determine the actual shock velocities and the conditions under which the radiative precursor appears. Future experiments will be designed to address these issues.

The authors would like to acknowledge the support of the OMEGA technical staff at the Laboratory for Laser Energetics and the target fabrication group at LLNL. This work was performed with funding from the U.S Department of Energy to the Univ. of Michigan under grants DE-FG03-99DP00284, DE-FG03-00SF22021, and to the Lawrence Livermore National Laboratory under contract No. W-7405-ENG48.

References

[1] L. Ensman and A. Burrows *et al*, Astrophys. J, **393**, 742 (1992).

[2] P. Ghavamian, *et al*, Astrophys. J, **535**, 266 (2000).

[3] R. S. Sutherland, G. V. Bicknell and M. A. Dopita, Astrophys. J, **414**, 510 (1993).

[4] B. Reipurth and J. Bally, Annu. Rev. Astron. Astrophys, **39**. 403 (2001).

[5] C. Feinstein, *et al*, Astrophys. J, **526**, 623 (1999).

[6] A. C. Raga, *et al*, Rev. Mex. AA, **35**, 123 (1999).

[7] J. C. Bozier, *et al*, Phys. Rev. Lett., **57**, 1304 (1986).

[8] Improved studies of such shocks in Xe shock tubes are now being conducted by M. Koenig and S. Bouquet and colleagues.

[9] C. A. Back, *et al.*, Phys. Rev. Lett., **84**, 274 (2000); D. Hoarty *et al*, Phys. Rev. Lett., **82**, 3070 (1999);

[10] M.J. Edwards, *et al.*, Phys. Rev. Lett., **87**, 85004 (2001); K. Shigemori, *et al.*, Astrophys. J., **533**, L159 (2000).

[11] T.S. Perry *et al.* Phys.Rev.Lett. **67**, 3784 (1991).

[12] C.A. Iglesias & F.J. Rogers, Astrophys. J. **464**, 943(1996); and references within.

[13] J. Larsen and S. M. Lane, J. Quant. Spect. Rad. Trans., **51**, 179 (1994).

[14] Y.B. Zeldovich and Y.P. Razier, *Physics of Shock Waves and High-Temperature Hydrodynamic Phenomena*, (Academic Press, New York, 1966).

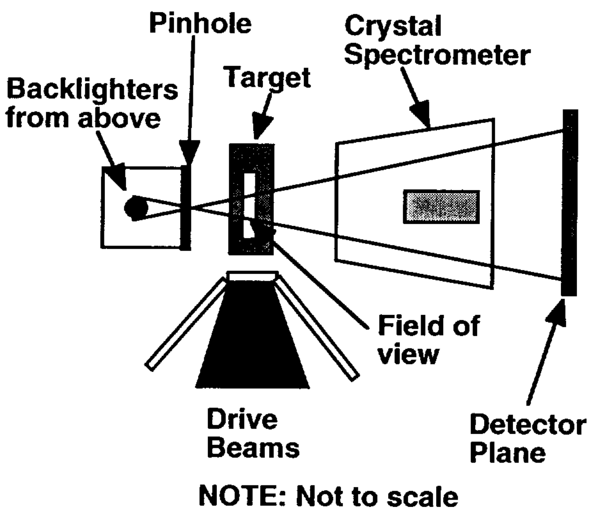

Figure 1: Keiter, Physical Review Letters

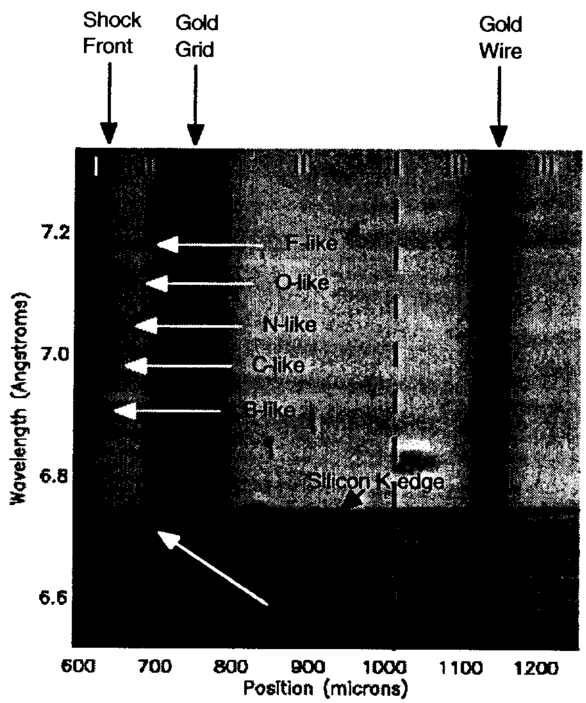

Figure 2a: Keiter, Physical Review Letters

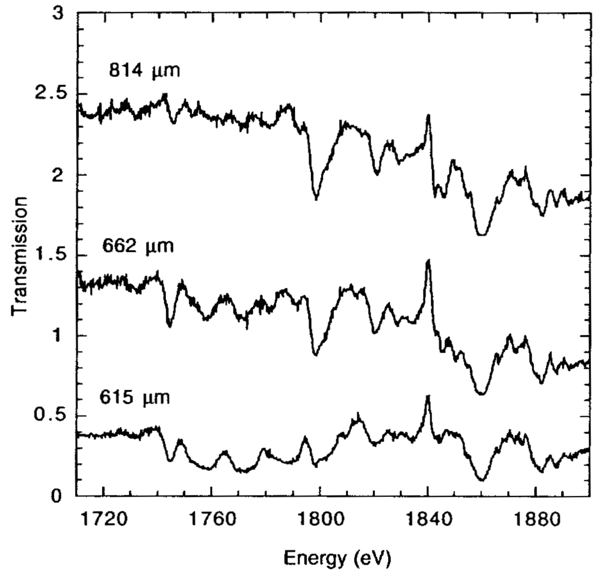

Figure 2b: Keiter, Physical Review Letters

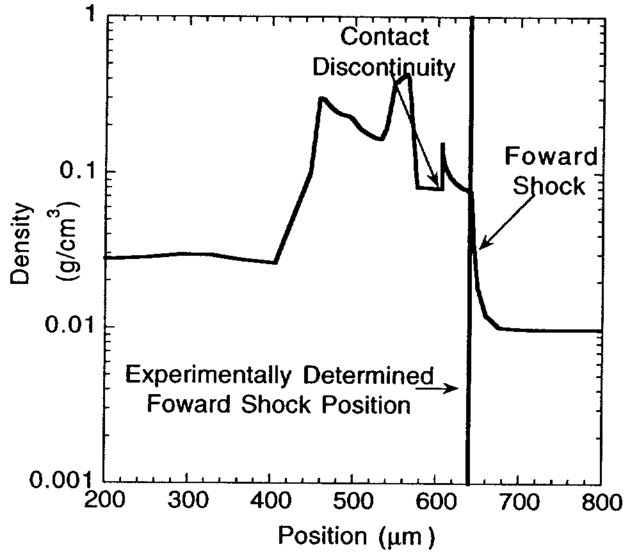

Figure 3: Keiter, Physical Review Letters

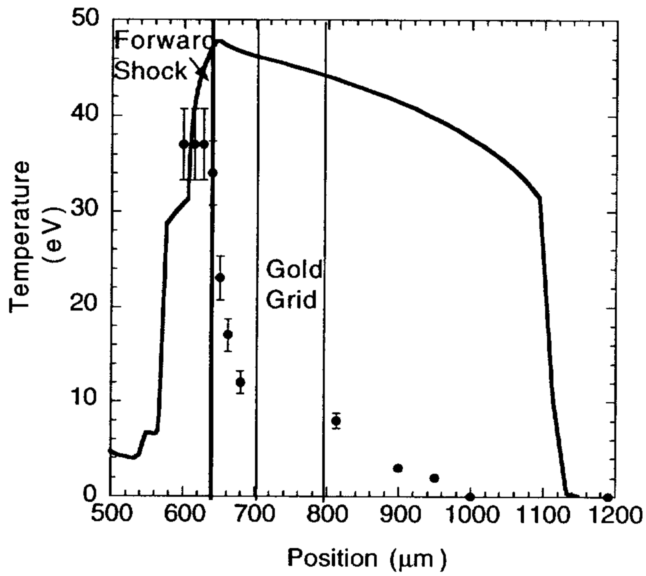

Figure 4: Keiter, Physical Review Letters

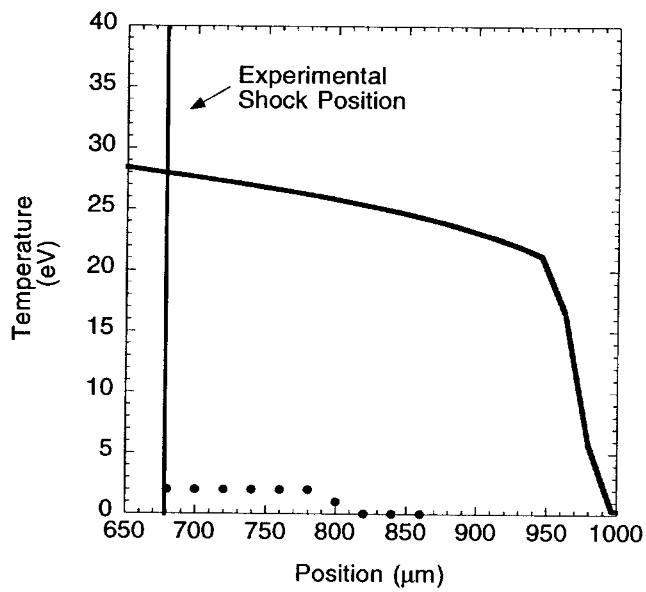

Figure 5: Keiter, Physical Review Letters

Figure Captions

Figure 1: Schematic of the experimental setup (not to scale). Drive beams strike a plastic slab, which hydrodynamically drives the radiative-precursor shock in the foam. Additional laser beams strike the backlighter, producing x-rays to diagnose the system.

Figure 2: a) A typical piece of data. Region I is shocked plastic, region II is the radiative precursor, and region III is cold, unshocked foam. Silicon absorption lines are present in regions I and II, and identified on the image. b) Vertical line-outs from three different positions from the previous image. The silicon absorption lines are identified on the image. As the line-outs progress deeper into the precursor region, the absorption lines become less prominent. The line-outs are offset in the vertical direction for visual purposes only.

Figure 3: A comparison of the HYADES density profile and the experimentally determined position of the forward shock.

Figure 4: A comparison between the experimentally determined temperature profile and the HYADES prediction of experimental parameters of 9.6 mg/cm^3 foam density and a laser intensity of 8.3 x 10^{14} W/cm^2. There is a large discrepancy between the experimental temperature profile and the HYADES simulations.

Figure 5: A comparison between the experimentally determined temperature profile and the HYADES prediction for the experimental parameters of 5 mg/cm^3 density foam and

3.4×10^{14} W/cm^2 laser intensity. The data indicate there is almost no radiative precursor, while the HYADES predictions suggest a much stronger radiative precursor should be present.